Paludification reduces black spruce growth rate but does not alter tree water use efficiency in Canadian boreal forested peatlands

Joannie Beaulne

Université du Québec à Montréal

Étienne Boucher

Université du Québec à Montréal

Michelle Garneau

Université du Québec à Montréal

Gabriel Magnan

Université du Québec à Montréal

Research

Keywords: black spruce growth, boreal biome, carbon allocation, ecophysiological mechanisms, forested peatland, paludification, stable isotope, water use efficiency

1 **Paludification reduces black spruce growth rate but does not alter tree**

2 **water use efficiency in Canadian boreal forested peatlands**

3 **Joannie Beaulne[1,2,3*], Étienne Boucher[1,2,4], Michelle Garneau[1,2,3,4], and Gabriel**

4 **Magnan[1,3]**

5 [1] Geotop Research Center, Université du Québec à Montréal, Montréal, Québec H3C 3P8, Canada

6 [2] Department of Geography, Université du Québec à Montréal, Montréal, Québec H3C 3P8,

7 Canada

8 [3] GRIL-UQAM, Université du Québec à Montréal, Montréal, Québec H3C 3P8, Canada

9 [4] Centre d'études nordiques, Université Laval, Québec, Québec G1V 0A6, Canada

11 * Email: joannie.beaulne@gmail.com

13 **Abstract**

14 **Background:** Black spruce (*Picea mariana* (Mill.) BSP)-forested peatlands are widespread

15 ecosystems in boreal North America in which peat accumulation, known as the paludification

16 process, has been shown to induce forest growth decline. However, the ecophysiological

17 mechanisms that lead to growth reductions in black spruce remain unexplored. Trees growing in

18 paludified forests have to deal with continuously evolving environmental conditions (e.g., water

19 table rise, increasing peat thickness) that may require growth mechanism adjustments over time. In

20 this study, we investigated tree ecophysiological mechanisms along a paludification gradient in a

21 boreal forested peatland of eastern Canada by combining peat-based and tree-ring analyses. Carbon

22 and oxygen stable isotopes in tree rings were used to document changes in carbon assimilation

23 rates, stomatal conductance, and water use efficiency. In addition, paleohydrological analyses were

24   performed to evaluate the dynamical ecophysiological adjustments of black spruce trees to site-

25   specific water table variations.

26   **Results:** Increasing peat accumulation considerably impacted forest growth, but no significant

27   differences in tree water use efficiency (iWUE) were observed between the study sites. Tree-ring

28   isotopic analysis indicates no iWUE decrease over the last 100 years, but rather an important

29   increase at each site up to the 1980s, before iWUE stabilized. Surprisingly, inferred basal area

30   increments did not reflect such trends. Our results suggest that the slower growth rates observed at

31   the most paludified sites are attributable, at least partially, to both lower carbon assimilation rates

32   and stomatal conductance. These findings show that iWUE variations do not necessarily reflect tree

33   ecophysiological adjustments required by changes in growing conditions. Local water table

34   variations induced no changes in ecophysiological mechanisms, but the synchronous shift in iWUE

35   observed at all sites in the mid-1980s suggests a tree response to regional or global factors, such as

36   increasing atmospheric CO_2 concentration.

37   **Conclusions:** Our study shows that paludification induces black spruce growth decline without,

38   however, altering tree water use efficiency in boreal forested peatlands. This is the first attempt in

39   exploring the complex interactions between stem growth, ecophysiological mechanisms, and

40   environmental conditions in paludified sites. Additional research on carbon allocation strategies is

41   of utmost importance to understand the carbon sink capacity of these widespread ecosystems and

42   better predict their response to future climate change.

43

44   **Keywords:** black spruce growth, boreal biome, carbon allocation, ecophysiological mechanisms,

45   forested peatland, paludification, stable isotope, water use efficiency

46

Background

Black-spruce (*Picea mariana* (Mill.) BSP)-dominated forested peatlands are widespread ecosystems in boreal North America (Korhola 1995; Crawford et al. 2003; Lavoie et al. 2005). In such environments, *Sphagnum* moss growth is favored and leads to the development of thick organic layers that maintain cool, acid, humid, and anaerobic soil conditions (Van Cleve et al. 1983; Fenton and Bergeron 2006). As this paludification process progresses, soil temperature and nutrients become limiting, and forest growth eventually declines (Boudreault et al. 2002; Harper et al. 2003; Simard et al. 2007; Lafleur et al. 2011), leading to tree dieback and an opening of forest stands. This negatively impacts the forest productivity and, therefore, several management practices have been developed to reduce or even reverse this process (e.g., Lavoie et al. 2005; Bergeron et al. 2007; Fenton et al. 2009). However, there is still a need to shed light on the mechanisms that control forest growth decline in paludified ecosystems in order to enhance our capacity to localize and anticipate the effects of paludification on forest productivity, and thus optimize management decisions.

While tree growth decline represents a well-established consequence of the paludification process, ecophysiological mechanisms that lead to growth reductions in black spruce remain unexplored. Based on existing ecophysiological theory (mostly developed in non-paludified sites), three mechanisms may possibly be invoked either jointly or separately to explain such declines. First, paludification process may reduce carbon assimilation rates (A), as it is well known that the photosynthesis apparatus of plants is sensitive to thermal (Göbel et al. 2019), oxygen (Bartholomeus et al. 2008) or nutrient limitations (Longstreth and Nobel 1980). A reduction in A would imply the downregulation of gross primary production (GPP) and less photosynthates export to stem growth. In temperate environments, such a positive relationship between GPP and stem growth has been elucidated (Belmecheri et al. 2014), but this relationship is far from being

72 applicable to boreal and paludified forests. In boreal environments, relationships between carbon

73 uptake and forest growth are either inconclusive (Rocha et al. 2006) or decoupled (Pappas et al.

74 2020), while remaining unexplored in paludified ecosystems. Second, growth decline could also

75 result from a reduction of stomatal conductance (g_s). When trees are severely affected by drought

76 stress, stomatal closure allows plants to reduce water losses during transpiration, but this

77 mechanism also penalizes carbon uptake and ultimately results in lower growth rates (Linares and

78 Camarero 2012). However, in paludified environments, adjustments of plant stomata to peat

79 accumulation, climate variability, and water table variations are yet to be determined. Lastly, trees

80 growing in nutrient-poor/low oxygen settings are more susceptible to allocate carbon to the root

81 system rather than to aboveground components (Giardina et al. 2003; Vicca et al. 2012). Thus,

82 changes in carbon allocation strategies favoring belowground biomass as peat accumulates could

83 explain the apparent growth decrease visible in stems.

84

85 Another source of uncertainties arises from the fact that trees growing in paludified ecosystems

86 have to deal with continuously evolving environmental conditions. The accumulation of thick

87 organic layers induces significant changes that highlight the dynamic interactions occurring in

88 boreal forested peatlands. For example, paludification is characterized by water table rise (Lavoie

89 et al. 2005; Fenton and Bergeron 2006), and interactions over time may exist between water table

90 fluctuations, stem growth, and tree water use efficiency (i.e., the ratio of carbon assimilated to water

91 losses through evapotranspiration; Farquhar et al. 1989). These interactions, which remains largely

92 unexplored, may vary in function of the degree of paludification (i.e., organic layer thickness).

93 Consequently, how growth mechanisms adjust to such changes and how they impact tree radial

94 growth over time needs to be addressed.

95

96 Carbon and oxygen stable isotopes in tree-ring cellulose may be of great help to disentangle

97 processes responsible for tree growth decline in paludified environments. Indeed, gas exchange

98   dynamics at the leaf-atmosphere interface are imprinted in the isotopic signature of annually-

99   produced wood. For example, both A and g_s affect carbon stable isotope fractionation in tree-ring

100   cellulose (Scheidegger et al. 2000; Cernusak et al. 2013), and the ratio between both, namely

101   intrinsic water use efficiency (iWUE=A/g_s), is at the core of ecosystem functioning (Guerrieri et al.

102   2019). Moreover, fractionation of oxygen stable isotopes reflects the magnitude of stomatal

103   controls (through g_s) on transpiration jointly with the signal of source water uptake (Barbour 2007).

104   Tree-ring based analysis of $\delta^{13}C$ and $\delta^{18}O$ can help tracking dynamical adjustments of

105   ecophysiological parameters to changing environmental conditions (Voelker et al. 2016). Such

106   strategies have been well studied for well-drained environments (Frank et al. 2015; Voelker et al.

107   2016), but have never been investigated for paludified sites. In addition, the use of a paleoecological

108   approach may be useful to investigate the interactions between tree growth mechanisms and local

109   environmental conditions in boreal forested peatlands. Analyses of peat cores are commonly used

110   to document, among others, past changes in both vegetation composition and hydrological

111   conditions. For example, testate amoeba (unicellular protists) shells preserved in peat are widely

112   used proxies for reconstructing variations in water table depths (Mitchell et al. 2008). Such

113   paleoecological and paleohydrological analyses have previously been conducted in forested

114   peatlands (Ruppel et al. 2013; Le Stum-Boivin et al. 2019; Magnan et al. 2019), but have never

115   been put in relation to tree growth.

116

117   In this study, we aim to improve our knowledge of the mechanisms that are driving tree growth

118   decline observed in black-spruce-dominated forested peatlands of eastern Canada. To do this, we

119   compare tree-ring-derived growth trends and stable-isotope-inferred ecophysiological processes

120   along a paludification gradient characterized by increasingly thicker peat deposits. More

121   specifically, the objectives of the study are to (1) determine whether the decline in stem growth

122   induced by the paludification process is attributable to changes in ecophysiological processes (such

123   as A or g_s) and/or to changes in carbon allocation strategies, and (2) evaluate the dynamical

ecophysiological adjustments to ever-changing environmental conditions. We hypothesised that (1)

growth decline results from a reduction of water use efficiency (iWUE), (2) reductions in iWUE

are greater in the most paludified sites, and (3) strongest ecophysiological adaptation also take place

in the most paludified sites. In order to test these hypotheses, we used an innovative approach that

combines peat-based paleohydrological analyses – to reconstruct past variations in water table

depth – and stable isotope analyses in tree rings – to investigate iWUE changes through time.

Methods

Study area

The study was conducted south of James Bay in eastern Canada, within the Clay Belt region part

of the black spruce-feather moss bioclimatic domain (Saucier et al. 2009; Fig. 1). This area is

particularly prone to paludification due to the relatively cold and humid climate, the flat

topography, and the dominance of poorly-drained clayey sediments left by the proglacial lakes

Barlow and Ojibway (Vincent and Hardy 1977). Mean annual temperature is 0.3°C (over the 1950-

2013 period), ranging from -18.9°C in January to 16.3°C in July, and mean annual precipitation is

818 mm (McKenney et al. 2011). The regional fire cycle is estimated at ~400 years since 1920

(Bergeron et al. 2004), allowing the accumulation of thick organic layers in forests between fire

events.
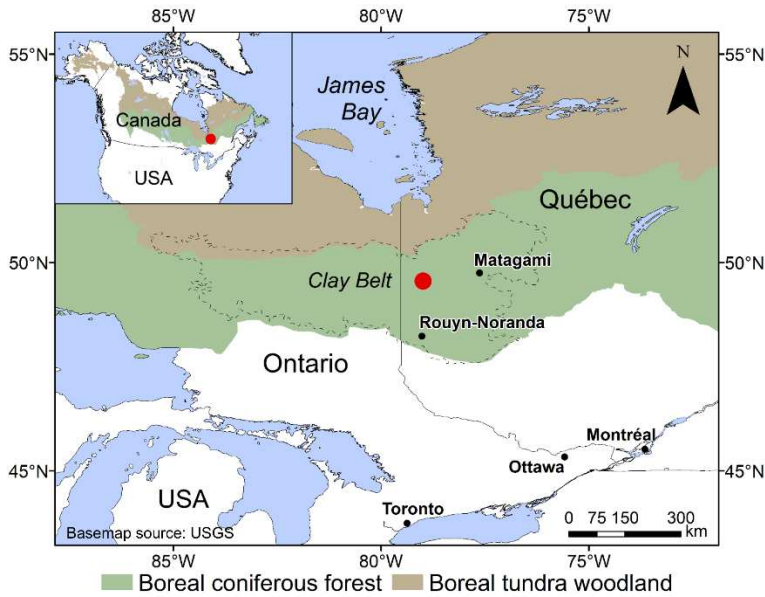
144

145 **Figure 1. Location of the studied Casa boreal forested peatland (red dot).**

146

147 **Site selection and sampling**

148 The Casa forested peatland (49°33'06"N, 78°59'10"O; Fig. S2.1) was selected following the studies

149 of Magnan et al. (2020) and Le Stum-Boivin et al. (2019) due to its regional representativeness in

150 terms of topography, vegetation composition, and canopy openness. The slope is <1% and the

151 organic layer thickness varies between 40 cm and more than 1 m along the selected transect. The

152 canopy cover is relatively closed but gradually opens up with organic layer thickening, which is

153 typically observed in forested peatlands of the Clay Belt. The aboveground vegetation is largely

154 dominated by black spruce and ericaceous shrubs, such as *Vaccinium angustifolium*, *Rhododendron*

155 *groenlandicum*, *Kalmia angustifolia*, and *Chamaedaphne calyculata*. The understory is dominated

156 by *Sphagnum* communities, particularly *S. angustifolium/fallax* under the tree canopy, and *S.*

157 *fuscum* where the canopy cover is more open.

158

159 Three sampling sites (CAS0, CAS50, CAS100) were established along a 100 m transect following

160 an organic matter thickness gradient within the selected forested peatland (Fig. 2). At each site, one

161 peat monolith was sampled down to the mineral contact using a Box corer (Jeglum et al. 1992).

162 Sampling locations were chosen to be representative of the degree of paludification of each site in

163 terms of peat thickness and canopy opening. Relative surface altitude and peat thickness were

164 measured at 5 m intervals along the transect using a high precision altimeter (ZIPLEVEL PRO-

165 2000) and an Oakfield probe. Water table depths were measured at the same intervals, in June 2017

166 and September 2018, a few hours after holes were dug to make sure that the water table level had

167 stabilized. Twenty black spruce trees were also sampled at each site within a 10 m radius of the

168 collected peat core. Only dominant and codominant trees with straight stems and no visible scars

169 were selected. Peat thickness was measured at the bottom of each sampled tree to validate the

170 concordance with the mean peat thickness of the site. The diameter at breast height (DBH) and the

171 height of selected trees were measured and cross-sections were collected at standard height (1.3 m).

172 The root system of one black spruce tree per site was excavated to verify the depth of the rooting

173 zone and the growth substrate (i.e., mineral or organic matter). Moreover, tree aboveground

174 biomass of each site was estimated by measuring the diameter at breast height (DBH) of all trees

175 (DBH ≥ 1 cm) within a 10×10 m plot and then using allometric equations adapted to black spruce

176 growth (Ung et al. 2008).

177
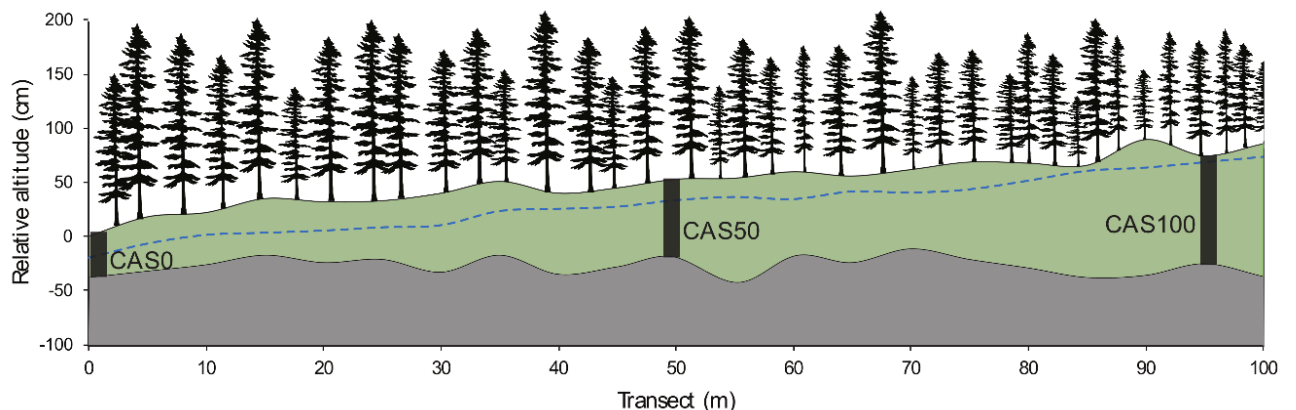
178

179 **Figure 2. Schematic of the three sites along the study transect.** Relative altitude of the organic

180 layer (green) and the mineral surface (grey) are shown. Black rectangles represent the location of

181 the sampled peat cores. The dotted blue line indicates the depth of the water table measured in the

182 field. Trees are not to scale but are representative of variations in canopy openness along the

183 transect.

184

185 **Black spruce radial growth analysis**

186 The sixty dried cross-sections were finely sanded (from 80 to 600 grit size) prior to ring-width

187 measurements along two radii using CooRecorder software (version 8.1.1; Larson 2016). Samples

188 were visually cross-dated using PAST5 software (version 5.0.610; Knibbe 2019), and skeleton plots

189 were generated using the R package *dplR* (version 1.6.9; Bunn et al. 2018). Ring-width series were

190 converted to annual basal area increment (BAI) to compare tree aboveground productivity between

191 the three sites, as BAI is more representative of three-dimensional stem growth than the linear ring-

192 width measurements (Husch et al. 2003; Biondi and Qeadan 2008). Individual BAI series were

193 produced using the R package *dplR* (version 1.6.9; Bunn et al. 2018), and yearly averages were

194 then calculated using all trees from the same site. Ring-width series were also standardized (Fig.

195 2.6) in order to perform correlation analyses with climate data (SM 1.1).

196

197 **Isotopic analysis of tree rings**

198 Black spruce ecophysiological processes were evaluated from carbon ($\delta^{13}C$) and oxygen ($\delta^{18}O$)

199 isotopic ratio analyses. These were performed on five trees per site and from two wood strips per

200 tree (i.e., a total of 30 samples). Sample preparation was carried out following the protocol

201 described in Giguère-Croteau et al. (2019) (SM 1.2). A five-year resolution over a 100-year period

202 (1919-2018) was considered. Alpha-cellulose was extracted, as suggested for black spruce samples

203 (Bégin et al. 2015), following the protocol used by Naulier et al. (2014).

204

205   Tree-ring $\delta^{13}C$ values vary according to discrimination against ^{13}C during photosynthesis, defined

206   as (Farquhar et al. 1982):

207

208
$$\Delta^{13}C = \frac{\delta^{13}C_{air} - \delta^{13}C_{tree}}{1 + (\delta^{13}C_{tree}/1000)},$$
(1)

209   where $\delta^{13}C_{air}$ is the carbon isotope ratio of the atmosphere and $\delta^{13}C_{tree}$ is the isotopic value of the

210   tree ring. $\delta^{13}C_{air}$ values were taken from McCarroll and Loader (2004) for the 1919-2003 period,

211   and were linearly extrapolated for the 2004-2018 period. Because of the five-year resolution of

212    $\delta^{13}C_{tree}$ values, we averaged the $\delta^{13}C_{air}$ values over five years. Following Farquhar et al. (1989),

213    $\Delta^{13}C$ is related to leaf intercellular CO_2 concentration (c_i) and ambient CO_2 concentration (c_a)

214   according to the following equation:

215

216
$$\Delta^{13}C = a + (b - a)\left(\frac{c_i}{c_a}\right),$$
(2)

217   where a (4.4‰) is the fractionation occurring during CO_2 diffusion through stomata (O'Leary

218   1981) and b (27‰) is the fractionation due to carboxylation by the Rubisco enzyme (Farquhar and

219   Richards 1984). Values of c_a were obtained from the Mauna Loa Observatory

220   (esrl.noaa.gov/gmd/ccgg/). Intrinsic water use efficiency (iWUE), defined as the amount of carbon

221   assimilated per unit of water lost, can then be estimated from c_i and c_a as follows (Ehleringer et al.

222   1993):

223

224
$$iWUE = \left(\frac{A}{g_s}\right) = \left(\frac{c_a - c_i}{1.6}\right),$$
(3)

225   where A is the rate of CO_2 assimilation, g_s is the stomatal conductance, and the constant 1.6

226   represents the ratio of water vapor and CO_2 diffusivity in air. Equation 3 shows that the difference

227   between c_a and c_i is related to the ratio of assimilation (A) to stomatal conductance (g_s).

228

229   Since the $\delta^{18}O$ composition of tree rings is mainly controlled by leaf water composition and

230   enrichment due to transpiration of lighter oxygen isotopes, $\delta^{18}O$ values are assumed to be related

231   to the stomatal conductance and independent of photosynthetic activity (Yakir 1992; Barbour

232   2007). Therefore, by combining $\delta^{13}C$ and $\delta^{18}O$ analyses it is possible to discriminate the effects of

233   changes in photosynthetic rate (A) and stomatal behavior (g_s) on iWUE (Scheidegger et al. 2000).

234

235   **Peat-based paleoecohydrological reconstructions**

236   In order to evaluate the response of black spruce ecophysiological mechanisms to hydrological

237   variations, water table depths were reconstructed from peat core analyses. The collected cores were

238   cut into 1 cm-thick slices before analysing testate amoeba assemblages at 1 cm intervals. Testate

239   amoeba shells were extracted following the standard protocol of Booth et al. (2010) (SM 1.3).

240   Samples were then analysed under an optical microscope (400× magnification). A minimum of 100

241   tests was counted per sample, except in highly humified peat samples, in which test concentration

242   was very low. In these cases, no water table depth (WTD) was inferred, as the total count (< 20

243   tests) was insufficient to ensure reliable WTD reconstruction (Payne and Mitchell 2009). Past

244   WTDs were reconstructed using a weighted average model with tolerance down-weighting and

245   inverse deshrinking (WA.inv.tol). The transfer function was built using the R package *rioja*

246   (version 0.9-15.1; Juggins 2017), from a modern dataset of 272 surface samples combining non-

247   forested (Lamarre et al. 2013) and forested peatlands (Beaulne et al. 2018 and this study) of eastern

248   Canada. High inferred WTD values corresponded to drier surface conditions.

249

250   Plant macrofossils and macroscopic charcoal particles (>0.5 mm) were also analysed along each

251   peat core to reconstruct vegetation dynamics since peat initiation and better understand the

252   paludification process at each site (SM 1.4).

253

254   **Peat core chronologies**

255   A total of 11 samples were submitted to A. E. Lalonde AMS Laboratory (University of Ottawa,

256   Canada) for accelerator mass spectrometry radiocarbon dating (^{14}C). Plant macrofossil remains

257   were carefully selected to date peat initiation, the last fire event, and main transitions in vegetation

258   composition at each sampling site (Beaulne et al. under review). The ^{14}C dates were calibrated

259   using the IntCal13 calibration curve (Reimer et al. 2013). ^{210}Pb dating was also achieved for the

260   uppermost 24-26 cm of peat cores at 1 cm intervals by alpha spectrometry (EGG Ortec 476A) at

261   the GEOTOP Research Center (Université du Québec à Montréal, Canada). Ages were inferred by

262   ^{210}Po activity measurement, using the constant rate of supply model (Appleby and Oldfield 1978)

263   following HNO_3-HCl-H_2O_2 sample digestion (Ali et al. 2008). Age-depth models were generated

264   using the *rbacon* package in R (version 2.3.9.1; Blaauw and Christen 2019). Ages are expressed in

265   calendar years before present (cal yr BP; 1950 CE) and the age of the peat surface is therefore set

266   to -67 cal yr BP (coring year: 2017 CE).

267

268   **Statistical analyses**

269   Statistical analyses were achieved to compare data in function of the degree of paludification. One-

270   way ANOVA analyses were performed to test for differences in BAIs, WTDs, δ^{13}C-derived

271   ecophysiological parameters, and tree-ring δ^{18}O between sites. In the case where dissimilarities

272   were observed between the study sites, multiple comparisons of means were further computed from

273   post-hoc Tukey HSD test to identify significant differences. Breakpoints in slopes were also

274   estimated from Davies test (Davies 1987) for δ^{13}C-derived ecophysiological parameters, tree-ring

275   δ^{18}O, and WTDs. All these statistical analyses were performed in R (R Core Team 2018).

276

277   **Results**

278   The study sites CAS0, CAS50, and CAS100 have an organic layer thickness of 40, 73, and 98 cm,

279   respectively (Table 1). Tree-ring analyses revealed even-aged stands covering the period 1839-

280   2018 CE at each site (see sample depth in Fig. 3 for tree age variability). Radiocarbon dating of the

281   most recent charcoal layer indicates that the last fire event occurred between 0 and 290 cal yr BP

282   (median age: 175-179 cal yr BP; Table S2.1). These results suggest that trees were from the first

283   cohort that grew after the last local fire, which most likely occurred around 200-250 years ago

284   (~1800 CE). The depth of the uppermost charcoal layer in the peat profile indicates that black

285   spruce established in a residual organic layer of 15, 45, and 65 cm at sites CAS0, CAS50, and

286   CAS100 respectively. The root system excavation of the three selected trees suggests that roots

287   reached the mineral soil at CAS0 and CAS50, but were restricted to the organic layer at CAS100.

288

289   **Table 1. Characteristics of the three study sites [a].**

Site	Mean organic layer thickness (cm)	Core length (cm)	Mean WTD (cm)	Mean DBH (cm)	Trees (*n*)	Tree aboveground biomass (kg m^{-2})	Tree density[b] (trees ha^{-1})	Mean tree height[c] (m)
CAS0	40±5	38	25±2	10.4±2.1	20	8.9±0.3	1200	13.8±0.4
CAS50	73±4	69	20±1	9.4±1.4	24	7.6±0.3	1200	11.3±0.5
CAS100	98±4	95	10±2	5.6±0.9	34	4.6±0.2	1000	10.4±0.5

290   [a] ± values correspond to standard errors.
291   [b] Include trees with a diameter at breast height (DBH) ≥ 9 cm.
292   [c] Calculated from the twenty black spruce trees (dominant and co-dominant) sampled at each site.
293

294   **Black spruce radial growth**

295   Tree height and DBH values decrease along the paludification gradient, with the lowest values

296   observed at the most paludified site (thickest organic layers) (Table 1). Mean DBHs of 10.4, 9.4,

297   and 5.6 cm were calculated for CAS0, CAS50, and CAS100, respectively. BAIs also indicate a

298   significant decrease in stem growth rates with increasing peat thickness (ANOVA F=53.97,

299   P<0.01; Fig. 3, S2.3). Trees from CAS0 added a greater wood surface with age, resulting in an

300   increasing BAI trend (mean BAI=70 mm^2). At CAS50, tree radial growth followed similar patterns

301   but was more limited (mean BAI=51 mm^2). In contrast, trees from CAS100 maintained relatively

302   constant BAI values, resulting in decreased wood production (mean BAI=40 mm^2). Estimates of

303   tree aboveground biomass showed similar trends with values of 8.9, 7.6, and 4.6 kg/m^2 for sites

304   CAS0, CAS50, and CAS100, respectively.

305
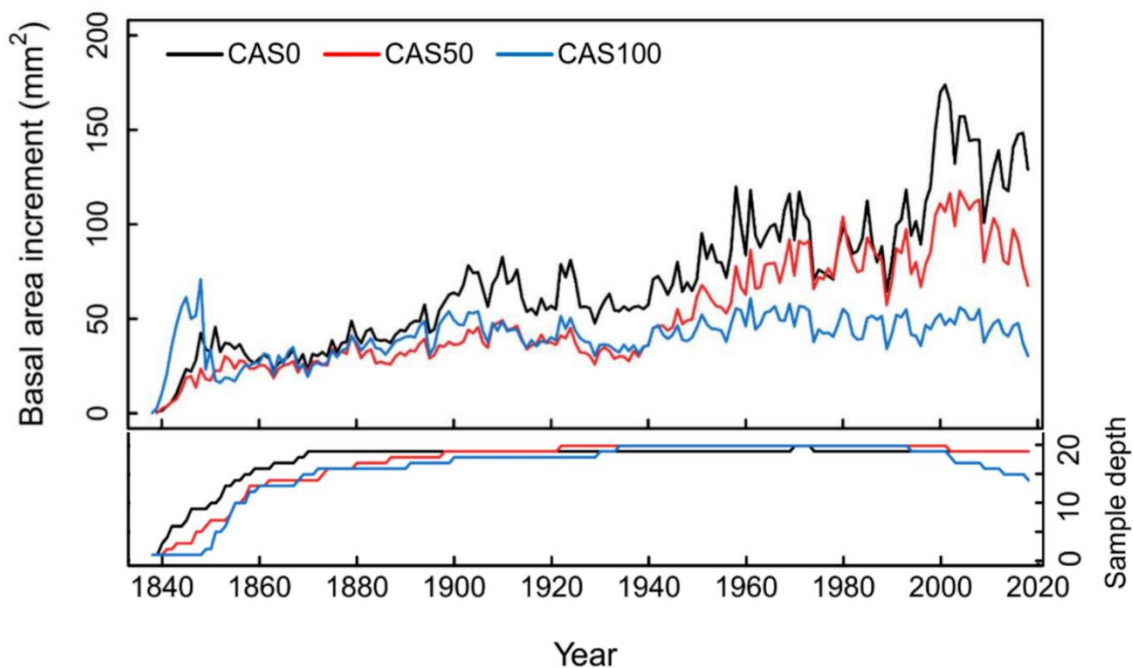
306

307   **Figure 3. Mean annual basal area increment of black spruce trees since their establishment**

308   **after the last fire event.** The decrease in sample depth (*n* trees) at CAS100 since 2000 is explained

309   by some trees for which the latest rings were partly absent. See Fig. S2.3 for BAI distribution.

310

311 **Trends in $\delta^{13}C$, $\delta^{18}O$, and iWUE**

312 The $\delta^{13}C$-derived ecophysiological parameters do not differ between the three sites over the 1919-

313 2000 period (Fig. 4a, ANOVAs $P>0.05$). Over time, black spruce trees used two different strategies

314 in response to rising c_a. A substantial increase in iWUE was first observed until the 1980s

315 ($c_a \approx 340$ ppm), along with relatively stable intercellular CO_2 concentration (c_i). During this

316 period, iWUE increased by 43% at each site. A major shift in tree ecophysiology then occurred in

317 the mid-1980s as c_i began to increase considerably (breakpoint=1984-1985, $P<0.01$). In parallel,

318 iWUE stabilized until 2018, except for at CAS0, where a new increase seems to have begun around

319 2000. However, this recent trend at CAS0 should be interpreted with caution considering its short

320 duration and the five-year resolution.

321

322 Tree-ring cellulose $\delta^{18}O$ analyses show no significant trends for the three sites across the whole

323 record (Fig. 4b, ANOVA $P<0.01$). However, oxygen stable isotope ratios were systematically

324 lower at the least paludified site (CAS0), suggesting a greater depletion in heavy isotopes (Tukey's

325 test $P<0.01$). For all series, tree-ring $\delta^{18}O$ values increased until ~1950 and became more constant

326 afterwards, except for a slightly decrease in the early 2000s at CAS50.

327
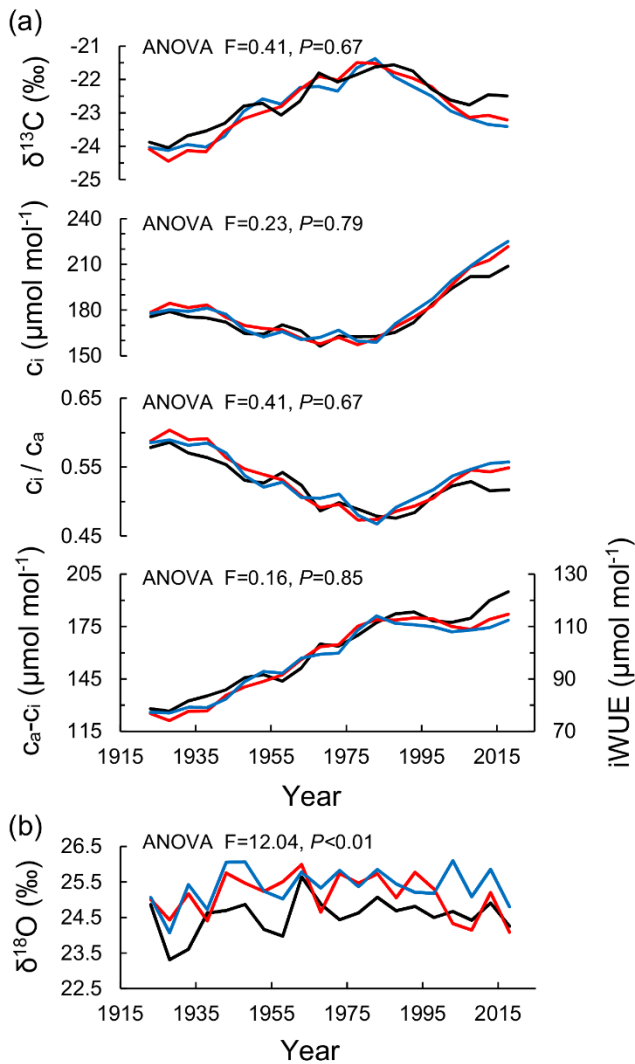
328

Figure 4. Black spruce ecophysiological response to rising c_α based on five-year resolution

δ^{13}C and δ^{18}O analyses for the period 1919-2018. (a) Tree-ring δ^{13}C and δ^{13}C-derived

ecophysiological parameter values (c_i, c_i/ c_a, c_a- c_i, iWUE); (b) tree-ring δ^{18}O values. Results from

CAS0, CAS50, and CAS100 are shown in black, red, and blue, respectively.

333

Paleoecohydrological reconstructions

Both hydrological conditions and vegetation composition were similar between the three sites

throughout the duration of black spruce growth (Fig. S2.4, S2.5). Macrofossil analysis showed that

the last fire (~1800 CE) induced a shift in vegetation composition from high dominance of woody

338   vegetation to a black spruce-*Sphagnum*-dominated stand (Fig. S2.3). The canopy opening allowed

339   rapid *Sphagnum* moss expansion in the bryophyte layer while the black spruce post-fire cohort

340   established.

341

342   Testate amoeba records indicate relatively wet conditions (high water table levels) shortly after the

343   fire, followed by a gradual lowering of the water table at the three sites (Fig. 5a, S2.5). Inferred

344   WTD values show very similar hydrological conditions at CAS50 and CAS100 during the post-

345   fire period (1840-2017). Both sites had stable WTD between 15 and 20 cm before water tables

346   deepened during the 2000s (breakpoint=2000, P<0.01), particularly in the very recent horizons

347   (~2010), while the water table lowered more gradually at CAS0 (breakpoint=1938, P<0.01). It

348   remains unclear whether the apparent drying trend reflects increasingly drier surface conditions or

349   simply an enhanced vertical growth of *Sphagnum* mosses that disconnected the peat surface from

350   the water table. Indeed, warmer conditions observed since the 1990s (Fig. S2.5) have led to

351   increasing growing degree days (Fig. 5b), which could have promoted this rapid peat accumulation.

352

353
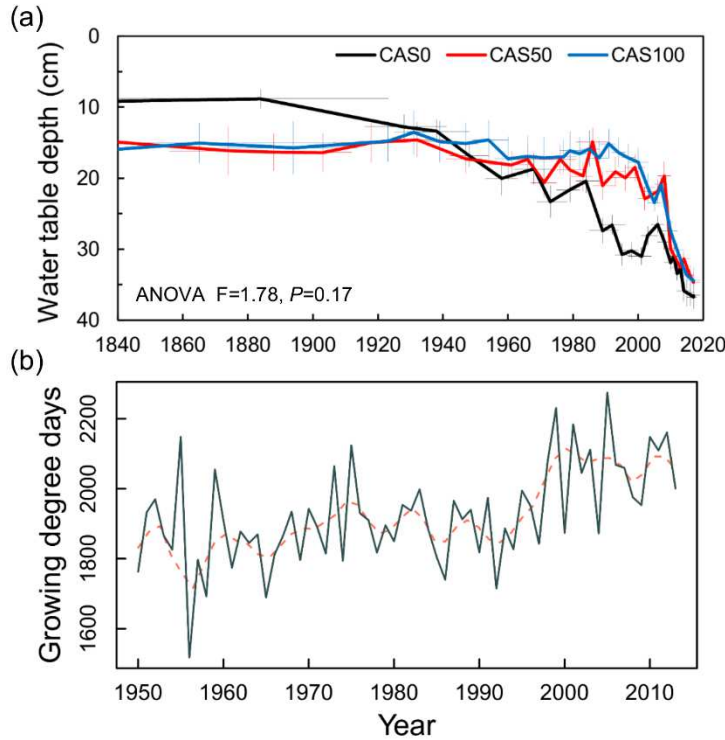
354

Figure 5. (a) WTD reconstructions for the post-fire period based on testate amoeba records and (b) growing degree days (>0°C) from May to September in the study area for the period 1950-2013. Error bars of both WTD reconstructions and age-depth modelling are shown by pale thin lines. Climate data were extracted from McKenney et al. (2011). A 10-year loess smoothing is shown by the pink dashed line.

360

Discussion

Stem growth decoupled from iWUE variations

Our study demonstrated that the paludification process considerably altered forest growth without, however, influencing the intrinsic water use efficiency of black spruce trees. Sites with the thickest organic matter accumulation were characterized by dominant trees that grew slower, presented smaller heights and diameters (DBH), and had a lower tree density comparatively to the least paludified site (Table 1; Fig. 3). These results are in agreement with previous studies that

368   documented forest productivity decline with increasing peat accumulation in the black spruce

369   feather moss domain of eastern Canada (e.g., Harper et al. 2003; Fenton et al. 2005; Lecomte et al.

370   2006; Simard et al. 2007). Surprisingly, however, our tree-ring stable isotope analysis indicates no

371   iWUE decrease over the last 100 years at the three study sites, but rather an important increase up

372   to the 1980s (Fig. 4a). Thus, contrary to our expectations, tree growth decline induced by the

373   paludification process does not result from a reduction in iWUE.

374

375   The stable isotope analysis revealed that δ^{13}C-derived parameters are almost identical in all sites

376   (no significant differences), both in terms of average iWUE levels and temporal variations,

377   suggesting that the ratio of assimilation rates to stomatal conductance is unaltered by the degree of

378   paludification. We thereby also refute our second research hypothesis. In order to maintain

379   comparable iWUE values across the paludification gradient (both in terms of mean and variability),

380   the proportionality of the A/g_s ratio needs to be preserved between sites. This implies that if A is

381   higher in the least paludified site (e.g., CAS0) and lower in the most paludified site (e.g., CAS100),

382   then g_s will adjust in such a way to maintain nearly identical A/g_s ratio, and consequently, iWUE

383   values. Actually, we suspect that this proportional adjustment in the A/g_s ratio might be an

384   important process driving interactions between iWUE and growth rates in a paludified context. As

385   a supporting evidence for this, we found that black spruce tree ring cellulose from the least

386   paludified site (CAS0) was significantly more depleted in ^{18}O compared to that of other sites (Fig.

387   4b). Unsurprisingly, CAS0 is also the site where radial growth rates are the highest. Increased

388   evapotranspiration rates are probably required to sustain enhanced carbon assimilation and growth

389   rates, forcing g_s to level up and proportionally adjust to increases in A (matching the ratio of other

390   sites). Consequently, higher evapotranspiration rates cause black spruce to pump more ^{18}O-depleted

391   water from soil depths (Evaristo et al. 2017), which in turn decreases the average δ^{18}O of tree ring

392   cellulose. Thus, the slower tree growth rates observed at the most paludified sites seem to result, at

393   least partially, from both lower carbon assimilation rates (A) and stomatal conductance (g_s).

394

These findings highlight that processes controlling radial tree growth are decoupled from those that
control gas exchanges (A and g_s), because of tree carbon use and allocation strategies. As an
example, many studies performed in non-paludified forests have shown that iWUE increases do
not directly translate into enhanced radial growth (e.g., Peñuelas et al. 2011; Lévesque et al. 2014;
van der Sleen et al. 2015; Giguère-Croteau et al. 2019). Based on a comparison of tree ring widths
and eddy-covariance flux towers in boreal Canada, Pappas et al. (2020) showed that aboveground
biomass, and most particularly radial stem growth, represents only a minor fraction (~9%) of the
total gross ecosystem production (GEP). Rocha et al. (2006) also found that stem growth, as
estimated from tree ring widths, was not correlated to eddy-covariance-derived GEP in the boreal
forest of central Manitoba. These findings point into the same direction: gas exchanges at the
vegetation-atmosphere interface are controlled at the leaf level, but the allocation of newly formed
photosynthates to either above or belowground compartments may depend on local growing
conditions and site-specific growth strategies. Our study must therefore be seen as an extreme case
where paludification induced locally-important edaphic changes that must have required tree
adaptation. Prioritization of belowground growth may have been more important in the most
paludified sites, neglecting carbon allocation to aboveground compartments. This allocation
strategy could reinforce tree anchoring (Nicoll et al. 2006) and enhance nutrient uptake (Vicca et
al. 2012; Fernández-Martínez et al. 2014), but further research is needed to shed light on the
processes driving allocation changes in black spruce trees.

Synchronous changes in iWUE over time

From the 1920s and until the 1980s, a ~40% iWUE increase was observed at each site, regardless
of the accumulated organic layer thickness. This important increase, which occurred over a short
period of time, is among the highest recorded; most studies report iWUE increases of 20-30% over

419   the last century (e.g., Peñuelas et al. 2011; Silva and Horwath 2013; Saurer et al. 2014; Frank et al.

420   2015; van der Sleen et al. 2015). The increased iWUE resulted from an active response of trees

421   characterized by the maintenance of a relatively constant c_i despite rising c_a.

422

423   Nevertheless, in the 1980s, tree response to rising c_a suddenly became passive, as shown by the

424   increasing c_i and the relatively constant c_a-c_i (iWUE) values at all sites (Fig. 4a). Likewise, a shift

425   to a passive response to increasing CO_2 concentration has previously been observed for various tree

426   species in the Canadian boreal forest (Giguère-Croteau et al. 2019; Marchand et al. 2020), in China

427   (Wang et al. 2012; Wu et al. 2015), and in Europe (Waterhouse et al. 2004; Gagen et al. 2011;

428   Linares and Camarero 2012). Three reasons might explain this shift in acclimation strategies.

429   Firstly, this finding possibly indicates reduced carbon assimilation rates (*A*). Indeed, in such poor

430   growing environments, the photosynthesis apparatus may saturate, and nutrient limitation may

431   downregulate the capacity of trees to assimilate atmospheric carbon (Tognetti et al. 2000; Saurer

432   et al. 2003). Secondly, WTD reconstructions indicate important changes in hydrological conditions

433   over the last 30 years (Fig. 5a) that might have altered black spruce iWUE. The recent water table

434   drawdown could have generated stressful growth conditions since black spruce develops

435   adventitious roots that are generally confined to the upper 20-30 cm of the organic layer (Lieffers

436   and Rothwell 1987; Viereck and Johnson 1990). However, such a drop in WTD would have most

437   certainly been accompanied by a reduction in stomatal conductance over time, which was not

438   observed here. Moreover, the apparent drying trend could simply reflect an enhanced vertical

439   *Sphagnum* moss growth, promoted by increasing growing degree days in the last decades (Fig. 5b;

440   Magnan et al. 2018; van Bellen et al. 2018; Primeau and Garneau, accepted; Robitaille et al.

441   accepted). The rapid accumulation of organic matter may have exceeded the capacity of

442   adventitious roots to develop higher in the soil profile, compromising the access to oxygen. Lastly,

443   considering that black spruce trees were approximately 180 years old in the 1980s, we cannot rule

444   out the stand age as another potential cause for the reduction in iWUE (Irvine et al. 2004; Kutsch

445   et al. 2009; Marchand et al. 2020). Further studies are needed to determine which of these factors

446   is mainly responsible for the significant shift observed in tree ecophysiological strategies in the

447   1980s.

448

449   **Ecophysiological adjustments to changing conditions**

450   Site-specific conditions have resulted in different tree growth rates along the paludification

451   gradient. As mention above, our results suggest that tree growth decline induced by peat

452   accumulation is related to lower carbon assimilation rates (A) and stomatal conductance (g_s) in the

453   most paludified sites, but also potentially to prioritization of carbon allocation to belowground

454   components. Therefore, changes in local environmental conditions have led to tree

455   ecophysiological adaptations, particularly in the most paludified sites. However, these adjustments

456   in growth mechanisms do not show in tree iWUE. The ratio A to g_s did not differ between sites,

457   despite differences in peat thickness, water table depth, tree rooting depth, canopy cover, and tree

458   growth rates (Table 1, Figs. 3, S2.2). These results indicate that iWUE variations do not necessarily

459   reflect tree ecophysiological adjustments induced by changing growing conditions.

460

461   The significant apparent water table lowering in the early 2000s at the three sites (Fig. 5a) did not

462   induce any changes in iWUE. The diverging WTD trend starting around 1940 at CAS0 neither

463   translated into a diverging iWUE trend. Although some important environmental factors were not

464   investigated (e.g., nutrients, soil temperature), these results suggest that site-specific conditions

465   were not determinant in iWUE variations. The synchronous shift in iWUE at the three sites in the

466   mid-1980s rather points out to a response to regional or global conditions, which were experienced

467   by trees from all sites. Likewise, Pearson correlations calculated between standardized ring-width

468   series and climate variables (monthly temperature and precipitation) indicate a shift in tree response

469   to climate in the 1980s (SM 1.1; Fig. S2.8). Black spruce trees became much less sensitive to both

470   temperatures and precipitation after 1980. The reduced sensitivity of trees to temperature since the

471   mid-twentieth century has been reported in previous tree ring studies of northern high-latitude

472   forests, and has been referred to as the "divergence problem" (e.g., Briffa et al. 2004; D'Arrigo et

473   al. 2008; Esper and Frank 2009; Schneider et al. 2014). This "divergence" phenomenon could

474   potentially be caused by thresholded responses or stresses induced by changes in growth conditions

475   (D'Arrigo et al. 2008). While further studies are required to shed light on such trends, these

476   observations could support the hypothesis of photosynthesis apparatus saturation. Indeed,

477   photosynthetic capacity, stimulated by elevated CO_2 concentration, may have been limited by the

478   poor growing conditions of forested peatlands, thus stabilizing iWUE and inhibiting stem growth

479   response to temperature.

480

481   **Conclusions**

482   In this study, we investigated the mechanisms that are driving tree growth decline in black-spruce-

483   dominated forested peatlands of eastern Canada, by combining dendrochronological,

484   paleoecological, and dendrogeochemical analyses. We attempted, for the first time, to unravel the

485   numerous and complex entanglements between paludification dynamics and forest ecophysiology

486   in these boreal ecosystems. Contrary to our expectations, tree growth decline induced by the

487   paludification process does not result from a reduction of water use efficiency (iWUE). Indeed, we

488   observed no significant differences in iWUE variations between the three study sites, which

489   reflected different degrees of paludification. A substantial increase in iWUE was even recorded at

490   each site for more than 50 years. Our tree-ring stable isotope analyses suggest that the decline in

491   forest growth with increasing peat accumulation is rather explained by lower assimilation rates (A),

492   together with lower stomatal conductance (g_s), and possibly by the prioritization of carbon

493   allocation to belowground components. Moreover, we found no evidence of tree ecophysiological

494 adaptations to variations in water table depth. However, a significant shift in tree ecophysiology

495 observed in the 1980s at all sites may suggest that the ratio between assimilation rates and stomatal

496 conductance (iWUE) is influenced by regional or global factors, such as climate or increasing

497 atmospheric CO_2 concentration. These findings illustrate the complexity of the interactions

498 between stem growth, ecophysiological processes, and environmental conditions, particularly in

499 paludified sites. These dynamics will need to be further investigated to better predict the response

500 of boreal forested peatlands to future climate change.

501

502 Our findings warrant further studies of vegetation/forest dynamics models and their application to

503 forested peatlands, as those models are often biased towards converting increases in iWUE into

504 increases in stem growth. A successful modelling of the c_i/c_a ratio based on the least-cost optimality

505 principle (Lavergne et al. 2020) would predict comparable iWUE trends, with correct implications

506 for gas exchanges at the leaf level, regardless of the degree of paludification. However, failing to

507 account for paludification-related carbon use and allocation strategies would result in the

508 overestimation of aboveground biomass production in sites where peat accumulation is substantial.

509 Peatlands are one the largest natural terrestrial ecosystems for carbon sequestration, and forested

510 peatlands represent a major component of these ecosystems in boreal regions (Thompson et al.

511 2016; Webster et al. 2018). Therefore, additional research on carbon allocation strategies is of

512 utmost importance to understand the carbon sink capacity of black-spruce-dominated boreal

513 ecosystems and make appropriate forest management decisions.

514

515 **Declarations**

516 **Acknowledgements**

517 We are grateful to Dr. Pierre Grondin (MFFP, Québec) for his precious contribution to this project.

518 Thanks to Nolann Chaumont and Camille Lepage for their help with field and laboratory work.

519   Special thanks to Dr. Nicole Sanderson (Geotop, UQAM) for her help with ^{210}Pb dating. We also

520   thank *Les Tourbeux.ses* for their help and useful advice. Thanks to Dr. David Paré (Canadian Forest

521   Service, NRCan) and Dr. Nicolas Bélanger (Université TELUQ) for their comments on an earlier

522   version of the manuscript, and to two anonymous reviewers for their constructive comments that

523   greatly helped improving the manuscript.

524

525   **Authors' contributions**

526   All authors designed the research and conducted the fieldwork. J.B. performed the research and

527   É.B., M.G. and G.M. helped analyzing the data. J.B. wrote the first draft of the manuscript and all

528   authors contributed critically to subsequent drafts and gave final approval for publication.

529

530   **Funding**

531   Scholarships to J.B. were provided by the Natural Sciences and Engineering Research Council of

532   Canada (NSERC-CGS M) and the Fonds de recherche du Québec – Nature et technologies

533   (FRQNT). Fieldwork and analyses were funded by the Natural Sciences and Engineering Research

534   Council of Canada through discovery grants to M.G. and É.B.

535

536   **Availability of data and materials**

537   Data will be archived on the Tree-Ring network of Qc-Lab database: http://dendro-qc-lab.ca

538

539   **Competing interests**

540   The authors declare no competing interests.

541

542   **Ethics approval and consent to participate**

543   Not applicable.

544

Consent for publication

Not applicable.

References

Ali AA, Ghaleb B, Garneau M, Asnong H, Loisel J (2008) Recent peat accumulation rates in minerotrophic peatlands of the Bay James region, Eastern Canada, inferred by ^{210}Pb and ^{137}Cs radiometric techniques. Appl Radiat Isot 66:1350-1358.

Appleby PG, Oldfield F (1978) The calculation of ^{210}Pb dates assuming a constant rate of supply of unsupported ^{210}Pb to the sediment. Catena 5:1-8.

Barbour MM (2007) Stable oxygen isotope composition of plant tissue: A review. Funct Plant Biol 34:83-94.

Bartholomeus RP, Witte JPM, van Bodegom PM, van Dam JC, Aerts R (2008) Critical soil conditions for oxygen stress to plant roots: Substituting the Feddes-function by a process-based model. J Hydrol 360:147-165.

Beaulne J, Garneau M, Magnan G, Boucher É (under review) Peat deposits store more carbon than trees in forested peatlands of the boreal biome. Scientific Reports.

Beaulne J, Magnan G, Garneau M (2018) Evaluating the potential of testate amoebae as indicators of hydrological conditions in boreal forested peatlands. Ecol Indic 91:386-394.

Bégin C, Gingras M, Savard MM, Marion J, Nicault A, Bégin Y (2015) Assessing tree-ring carbon and oxygen stable isotopes for climate reconstruction in the Canadian northeastern boreal forest. Palaeogeogr Palaeoclimatol Palaeoecol 423:91-101.

566   Belmecheri S, Maxwell RS, Taylor AH, Davis KJ, Freeman KH, Munger WJ (2014) Tree-ring δ^{13}C

567   tracks flux tower ecosystem productivity estimates in a NE temperate forest. Environ Res Lett 9:

568   074011 (9pp).

569   Bergeron Y, Drapeau P, Gauthier S, Lecomte N (2007) Using knowledge of natural disturbances

570   to support sustainable forest management in the northern Clay Belt. For Chron 83:326-337.

571   Bergeron Y, Gauthier S, Flannigan MD, Kafka V (2004) Fire regimes at the transition between

572   mixedwood and coniferous boreal forest in northwestern Quebec. Ecology 85:1916-1932.

573   Biondi F, Qeadan F (2008) A theory-driven approach to tree-ring standardization: defining the

574   biological trend from expected basal area increment. Tree Ring Res 64:81-96.

575   Blaauw M, Christen JA (2019) rbacon: Age-Depth Modelling using Bayesian Statistics. R package

576   version 2.3.9.1. https://CRAN.R-project.org/package=rbacon

577   Booth RK, Lamentowicz M, Charman DJ (2010) Preparation and analysis of testate amoebae in

578   peatland palaeoenvironmental studies. Mires Peat 7:1-7.

579   Boudreault C, Bergeron Y, Gauthier S, Drapeau P (2002) Bryophyte and lichen communities in

580   mature to old-growth stands in eastern boreal forests of Canada. Can J For Res 32:1080-1093.

581   Briffa KR, Osborn TJ, Schweingruber FH (2004) Large-scale temperature inferences from tree

582   rings: a review. Glob Planet Change 40:11-26.

583   Bunn A, Korpela M, Biondi F, Campelo F, Mérian P, Qeadan F, … Wernicke J (2018) dplR:

584   Dendrochronology Program Library in R. R package version 1.6.9. https://CRAN.R-

585   project.org/package=dplR

586   Cernusak LA, Ubierna N, Winter K, Holtum JAM, Marshall JD, Farquhar GD (2013)

587   Environmental and physiological determinants of carbon isotope discrimination in terrestrial

588   plants. New Phytol 200:950-965.

589   Crawford RMM, Jeffree CE, Rees WG (2003) Paludification and forest retreat in northern oceanic

590   environments. Ann Bot 91:213-226.

591   D'Arrigo R, Wilson R, Liepert B, Cherubini P (2008) On the 'Divergence Problem' in Northern

592   Forests: A review of the tree-ring evidence and possible causes. Glob Planet Change 60:289-305.

593   Davies RB (1987) Hypothesis testing when a nuisance parameter is present only under the

594   alternative. Biometrika 74:33-43.

595   Ehleringer JR, Hall AE, Farquhar GD (1993) Stable isotopes and plant carbon–water relations.

596   Academic Press, New York.

597   Esper J, Frank D (2009) Divergence pitfalls in tree-ring research. Clim Change 94:261-266.

598   Evaristo J, McDonnell JJ, Clemens J (2017) Plant source water apportionment using stable

599   isotopes: A comparison of simple linear, two-compartment mixing model approaches. Hydrol

600   Process 31:3750-3758.

601   Farquhar GD, Ehleringer JR, Hubick KT (1989) Carbon isotope discrimination and photosynthesis.

602   Annu Rev Plant Physiol 40:503-537.

603   Farquhar GD, O'Leary MH, Berry JA (1982) On the relationship between carbon isotope

604   discrimination and the intercellular carbon dioxide concentration in leaves. Aust J Plant Physiol

605   9:121-137.

606   Farquhar GD, Richards RA (1984) Isotopic composition of plant carbon correlates with water-use

607   efficiency of wheat genotypes. Aust J Plant Physiol 11:539-552.

608   Fenton N, Bergeron Y (2006) Facilitative succession in a boreal bryophyte community driven by

609   changes in available moisture and light. J Veg Sci 17:65-76.

610   Fenton N, Lecomte N, Légaré S, Bergeron Y (2005) Paludification in black spruce (*Picea mariana*)

611   forests of eastern Canada: Potential factors and management implications. For Ecol Manag

612   213:151-159.

613   Fenton NJ, Simard M, Bergeron Y (2009) Emulating natural disturbances: the role of silviculture

614   in creating even-aged and complex structures in the black spruce boreal forest of eastern North

615   America. J For Res 14:258-267.

616   Fernández-Martínez M, Vicca S, Janssens IA, Sardans J, Luyssaert S, Campioli M, … Peñuelas, J

617   (2014) Nutrient availability as the key regulator of global forest carbon balance. Nat Clim Change

618   4:471-476.

619   Frank DC, Poulter B, Saurer M, Esper J, Huntingford C, Helle G, … Weigl M (2015) Water-use

620   efficiency and transpiration across European forests during the Anthropocene. Nat Clim Change

621   5:579-583.

622   Gagen M, Finsinger W, Wagner-Cremer F, Mccarroll D, Loader NJ, Robertson I, … Kirchhefer A

623   (2011) Evidence of changing intrinsic water-use efficiency under rising atmospheric CO_2

624   concentrations in Boreal Fennoscandia from subfossil leaves and tree ring $\delta^{13}C$ ratios. Glob Change

625   Biol 17:1064-1072.

626   Giardina CP, Ryan MG, Binkley D, Fownes JH (2003) Primary production and carbon allocation

627   in relation to nutrient supply in a tropical experimental forest. Glob Change Biol 9:1438-1450.

628   Giguère-Croteau C, Boucher É, Bergeron Y, Girardin MP, Drobyshev I, Silva LCR, … Garneau

629   M (2019) North America's oldest boreal trees are more efficient water users due to increased

630   [CO2], but do not grow faster. Proc Natl Acad Sci USA 116:2749-2754.

631   Göbel L, Coners H, Hertel D, Willinghöfer S, Leuschner C (2019) The Role of Low Soil

632   Temperature for Photosynthesis and Stomatal Conductance of Three Graminoids From Different

633   Elevations. Front Plan Sci 10:330. https://doi.org/10.3389/fpls.2019.00330

634   Guerrieria R, Belmecheri S, Ollinger SV, Asbjornsen H, Jennings K, Xiao J, … Richardson AD

635   (2019) Disentangling the role of photosynthesis and stomatal conductance on rising forest water-

636   use efficiency. Proc Natl Acad Sci USA 116:16909-16914.

637   Harper K, Boudreault C, DeGrandpré L, Drapeau P, Gauthier S, Bergeron Y (2003) Structure,

638   composition, and diversity of old-growth black spruce forest of the Clay Belt region in Quebec and

639   Ontario. Environ Rev 11:S79-S98.

640   Husch B, Beers TW, Kershaw Jr JA (2003) Forest Mensuration (4th ed.). John Wiley & Sons, New

641   York.

642   Irvine J, Law BE, Kurpius MR, Anthoni PM, Moore D, Schwarz PA (2004) Age-related changes

643   in ecosystem structure and function and effects on water and carbon exchange in ponderosa pine.

644   Tree Physiol 24:753-763.

645   Jeglum JK, Rothwell RL, Berry GJ, Smith GKM (1992) A Peat Sampler for Rapid Survey.

646   Frontline, Technical Note 13 921-932. Canadian Forestry Service, Sault-Sainte-Marie.

647   Juggins S (2017) rioja: Analysis of Quaternary Science Data. R package version 0.9-15.1.

648   http://cran.r-project.org/package=rioja

649   Knibbe B (2019) PAST5: Personal Analysis System for Tree Ring Research version 5.0.610.

650   Viennes: SCIEM. http://www.sciem.com/products/past/

651   Korhola A (1995) Holocene climatic variations in southern Finland reconstructed from peat-

652   initiation data. Holocene 5:43-58.

653   Kutsch WL, Wirth C, Kattge J, Nöllert S, Herbst M, Kappen L (2009) Ecophysiological

654   characteristics of mature trees and stands – consequences for old-growth forest productivity. In C

655   Wirth, G Gleixner, M Heimann (Eds.) Old-Growth Forests – Function, Fate and Value. Springer-

656   Verlag, Heidelberg.

657   Lafleur B, Paré D, Fenton NJ, Bergeron Y (2011) Growth and nutrition of black spruce seedlings

658   in response to disruption of Pleurozium and Sphagnum moss carpets in boreal forested peatlands.

659   Plant Soil 345:141-153.

660   Lamarre A, Magnan G, Garneau M, Boucher É (2013) A testate amoeba-based transfer function

661   for paleohydrological reconstruction from boreal and subarctic peatlands in northeastern Canada.

662   Quat Int 306:88-96.

663   Larson L-A (2016) CooRecorder: image co-ordinate recording, version 8.1.1 Saltsjöbaden: Cybis.

664   http://www.cybis.se

665   Lavergne A, Voelker S, Csank A, Graven H, de Boer HJ, Daux V, … Prentice IC (2020) Historical

666   changes in the stomatal limitation of photosynthesis: empirical support for an optimality principle.

667   New Phytol 225:2484-2497.

668   Lavoie M, Paré D, Fenton N, Groot A, Taylor K (2005) Paludification and management of forested

669   peatlands in Canada: a literature review. Environ Rev 13 :21-50.

670   Le Stum-Boivin É, Magnan G, Garneau M, Fenton NJ, Grondin P, Bergeron Y (2019)

671   Spatiotemporal evolution of paludification associated with autogenic and allogenic factors in the

672   black spruce–moss boreal forest of Québec, Canada. Quat Res 91:650-664.

673   Lecomte N, Simard M, Bergeron Y (2006) Effects of fire severity and initial tree composition on

674   stand structural development in the coniferous boreal forest of northwestern Québec, Canada.

675   Écoscience 13:152-163.

676   Lévesque M, Siegwolf R, Saurer M, Eilmann B, Rigling A (2014) Increased water-use efficiency

677   does not lead to enhanced tree growth under xeric and mesic conditions. New Phytol 203:94-109.

678   Lieffers VJ, Rothwell RL (1987) Rooting of peatland black spruce and tamarack in relation to depth

679   of water table. Can J Bot 65:817-821.

680   Linares JC, Camarero JJ (2012) From pattern to process: linking intrinsic water-use efficiency to

681   drought-induced forest decline. Glob Change Biol 18:1000-1015.

682   Longstreth DJ, Nobel PS (1980) Nutrient influences on leaf photosynthesis: Effects of nitrogen,

683   phosphorus, and potassium for *Gossypium Hirsutum* L. Plant Physiol 65:541-543.

684   Magnan G, Garneau M, Le Stum-Boivin É, Grondin P, Bergeron Y (2020) Long-term carbon

685   sequestration in boreal forested peatlands in eastern Canada. Ecosystems.

686   https://doi.org/10.1007/s10021-020-00483-x

687   Magnan G, Le Stum-Boivin É, Garneau M, Grondin P, Fenton N, Bergeron Y (2019) Holocene

688   vegetation dynamics and hydrological variability in forested peatlands of the Clay Belt, eastern

689   Canada, reconstructed using a palaeoecological approach. Boreas 48:131-146.

690   Magnan G, van Bellen S, Davies L, Froese D, Garneau M, Mullan-Boudreau G, …Shotyk S (2018)

691   Impact of the Little Ice Age cooling and 20th century climate change on peatland vegetation

692   dynamics in central and northern Alberta using a multi-proxy approach and high-resolution peat

693   chronologies. Quat Sci Rev 185:230-243.

694   Marchand W, Gigardin MP, Hartmann H, Depardieu C, Isabel N, Gauthier S, … Bergeron Y (2020)

695   Strong overestimation of water-use efficiency responses to rising CO_2 in tree-ring studies. Glob

696   Change Biol. https://doi.org/10.1111/gcb.15166

697   McCarroll D, Loader NJ (2004) Stable isotopes in tree rings. Quat Sci Rev 23:771-801.

McKenney DW, Hutchinson MF, Papadopol P, Lawrence K, Pedlar J, Campbell K, … Owen T (2011) Customized spatial climate models for North America. Bull Am Meteorol Soc December 1612-1622.

Mitchell EAD, Charman DJ, Warner BG (2008) Testate amoebae analysis in ecological and paleoecological studies of wetlands: past, present and future. Biodivers Conserv 17:2115-2137.

Naulier N, Savard MM, Bégin C, Marion J, Arseneault D, Bégin Y (2014) Carbon and oxygen isotopes of lakeshore black spruce trees in northeastern Canada as proxies for climatic reconstruction. Chem Geol 374-375:7-43.

Nicoll BC, Gardiner BA, Rayner B, Peace AJ (2006) Anchorage of coniferous trees in relation to species, soil type, and rooting depth. Can J For Res 36:1871-1883.

O'Leary MH (1981) Carbon isotope fractionation in plants. Phytochemistry 20:553-567.

Pappas C, Maillet J, Rakowski S, Baltzer JL, Barr AG, Black TA, ... Sonnentag O (2020) Aboveground tree growth is a minor and decoupled fraction of boreal forest carbon input. Agric For Meteorol 290:108030.

Payne RJ, Mitchell EAD (2009) How many is enough? Determining optimal count totals for ecological and palaeoecological studies of testate amoebae. J Paleolimnol 42:483-495.

Peñuelas J, Canadell JG, Ogaya R (2011) Increased water-use efficiency during the 20th century did not translate into enhanced tree growth. Glob Ecol Biogeogr 20:597-608.

Primeau P, Garneau M. (accepted) Carbon accumulation in peatlands following a boreal to subarctic gradient in eastern Canada. Holocene.

R Core Team (2018) R: A language and environment for statistical computing, version 3.5.5. Viennes: R Foundation for Statistical Computing. https://www.r-project.org/

720   Reimer PJ, Bard E, Bayliss A, Beck JW, Blackwell PG, Bronk Ramsey C, … van der Plicht J

721   (2013) IntCal13 and MARINE13 radiocarbon age calibration curves 0-50000 years calBP.

722   Radiocarbon 55:1869-1887.

723   Robitaille M, Garneau M, van Bellan S, Sanderson NK (accepted). Long-term and recent

724   ecohydrological dynamics of patterned peatlands in north-central Quebec. Holocene.

725   Rocha AV, Goulden ML, Dunn AL, Wofsy SC (2006) On linking interannual tree ring variability

726   with observations of whole-forest CO_2 flux. Glob Change Biol 12:1378-1389.

727   Ruppel M, Väliranta M, Virtanen T, Korhola A (2013) Postglacial spatiotemporal peatland

728   initiation and lateral expansion dynamics in North America and northern Europe. Holocene

729   23:1596-1606.

730   Saucier J-P, Robitaille A, Grondin P (2009) Cadre bioclimatique du Québec. In R Doucet, M Côté

731   (Eds.) Manuel de foresterie, 2nd edn. Éditions MultiMondes, Québec.

732   Saurer M, Cherubini P, Bonani G, Siegwolf R (2003) Tracing carbon uptake from a natural CO2

733   spring into tree rings: an isotope approach. Tree Physiol 23:997-1004.

734   Saurer M, Spahni R, Frank DC, Joos F, Leuenberger M, Loader NJ, … Young GHF (2014) Spatial

735   variability and temporal trends in water-use efficiency of European forests. Glob Change Biol

736   20:3700-3712.

737   Scheidegger Y, Saurer M, Bahn M, Siegwolf R (2000) Linking stable oxygen and carbon isotopes

738   with stomatal conductance and photosynthetic capacity: a conceptual model. Oecologia 125:350-

739   357.

740   Schneider L, Esper J, Timonen M, Büntgen U (2014) Detection and evaluation of an early

741   divergence problem in northern Fennoscandian tree-ring data. Oikos 123:559-566.

742 Silva LCR, Horwath WR (2013) Explaining Global Increases in Water Use Efficiency: Why Have

743 We Overestimated Responses to Rising Atmospheric CO2 in Natural Forest Ecosystems? PloS one

744 8:e53089 (5p).

745 Simard M, Lecomte N, Bergeron Y, Bernier PY, Paré D (2007) Forest productivity decline caused

746 by successional paludification of boreal soils. Ecol Appl 17:1619-1637.

747 Thompson DK, Simpson BN, Beaudoin A (2016) Using forest structure to predict the distribution

748 of treed boreal peatlands in Canada. For Ecol Manag 372:19-27.

749 Tognetti T, Cherubini P, Innes JL (2000) Comparative stem-growth rates of Mediterranean trees

750 under background and naturally enhanced ambient CO_2 concentrations. New Phytol 146:59-74.

751 Ung CH, Bernier P, Guo XJ (2008) Canadian national biomass equations: new parameter estimates

752 that include British Columbia data. *Can J For Res* 38:1123–1132.

753 van Bellen S, Magnan G, Davies L, Froese D, Mullan-Boudreau G, Zaccone C, … Shotyk W (2018)

754 Testate amoeba records indicate regional 20th-century lowering of water tables in ombrotrophic

755 peatlands in central-northern Alberta, Canada. Glob Change Biol 24:2758-2774.

756 Van Cleve K, Dyrness CT, Viereck LA, Fox J, Chapin FS, Oechel W (1983) Taiga ecosystems in

757 interior Alaska. BioScience 33:39-44.

758 van der Sleen P, Groenendijk P, Vlam M, Anten NPR, Boom A, Bongers F, … Zuidema PA (2015)

759 No growth stimulation of tropical trees by 150 years of CO_2 fertilization but water-use efficiency

760 increased. Nat Geosci 8:24-28.

761 Vicca S, Luyssaert S, Peñuelas J, Campioli M, Chapin FS, Ciais P, … Janssens IA (2012) Fertile

762 forests produce biomass more efficiently. Ecol Lett 15:520-526.

763 Viereck LA, Johnston WF (1990) *Picea mariana* (Mill.) B.S.P. In RM Burns & BH Honkala (Eds.)

764 Silvics of North America: 1. Conifers. US Department of Agriculture. Forest Service, Washington.

765 Vincent J-S, Hardy L (1977) L'évolution et l'extension des lacs glaciaires Barlow et Ojibway en

766 territoire québécois. Géo Phy Quat 31:357-372.

767 Voelker SL, Brooks JR, Meinzer FC, Anderson R, Bader MKF, Battipaglia G, … Wingate L (2016)

768 A dynamic leaf gas-exchange strategy is conserved in woody plants under changing ambient CO2:

769 evidence from carbon isotope discrimination in paleo and CO2 enrichment studies. Glob Change

770 Biol 22:889-902.

771 Wang W, Liu X, An W, Xu G, Zeng X (2012) Increased intrinsic water-use efficiency during a

772 period with persistent decreased tree radial growth in northwestern China: Causes and implications.

773 For Ecol Manag 275:14-22.

774 Waterhouse JS, Switsur VR, Barker AC, Carter AHC, Hemming DL, Loader NJ, Robertson I

775 (2004) Northern European trees show a progressively diminishing response to increasing

776 atmospheric carbon dioxide concentrations. Quat Sci Rev 23:803-810.

777 Webster K, Bhatti JS, Thompson DK, Nelson SA, Shaw CH, Bona KA, … Kurz WA (2018)

778 Spatially-integrated estimates of net ecosystem exchange and methane fuxes from Canadian

779 peatlands. Carbon Balance Manag 13:1-21.

780 Wu G, Liu X, Chen T, Xu G, Wang W, Zeng X, Zhang X (2015) Elevation-dependent variations

781 of tree growth and intrinsic water-use efficiency in Schrenk spruce (*Picea schrenkiana*) in the

782 western Tianshan Mountains, China. Front Ecol Evol 6:309.

783 Yakir D (1992) Variations in the natural abundance of oxygen-18 and deuterium in plant

784 carbohydrates. Plant Cell Environ 15:1005-1020.

Figures
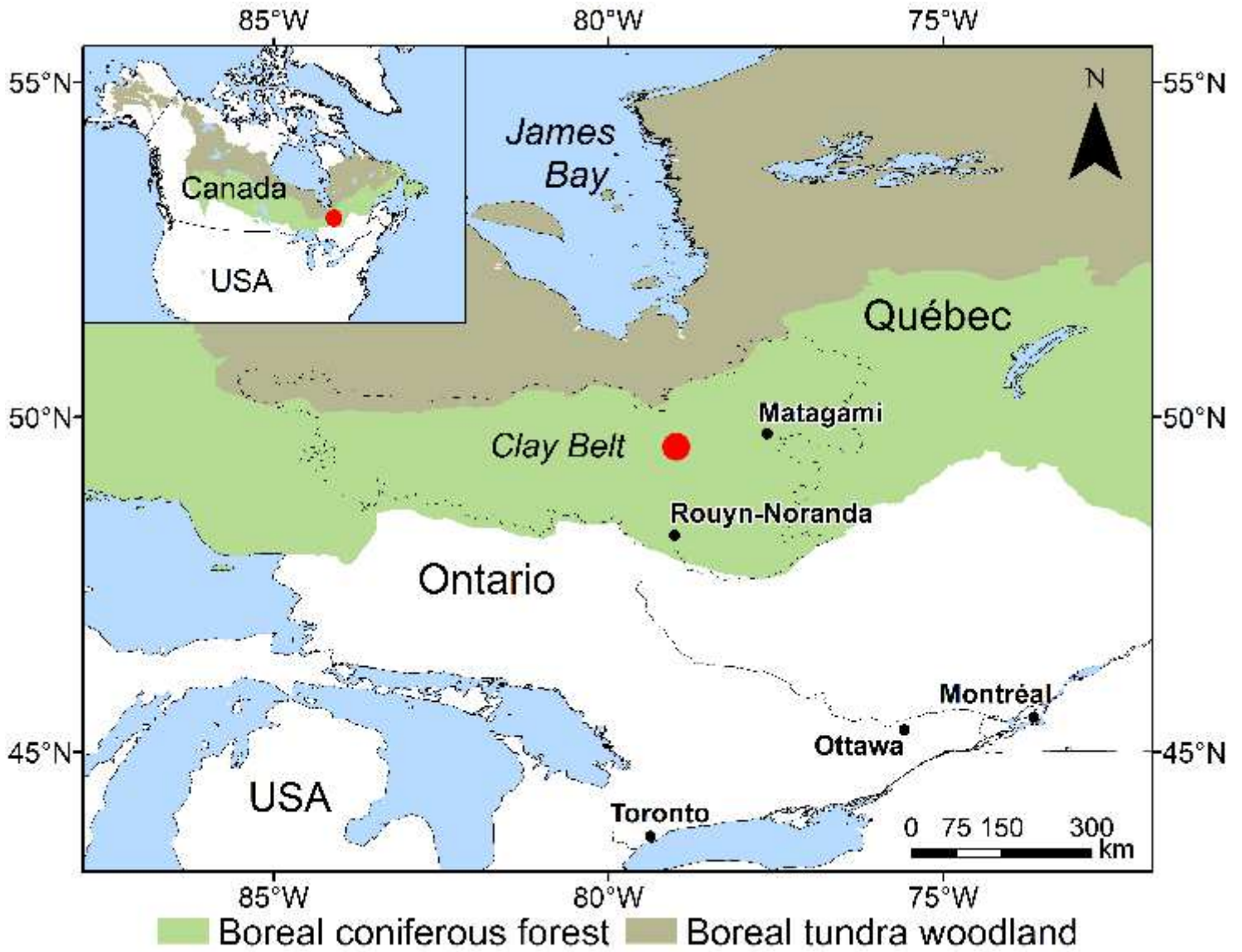
Figure 1

Location of the studied Casa boreal forested peatland (red dot).
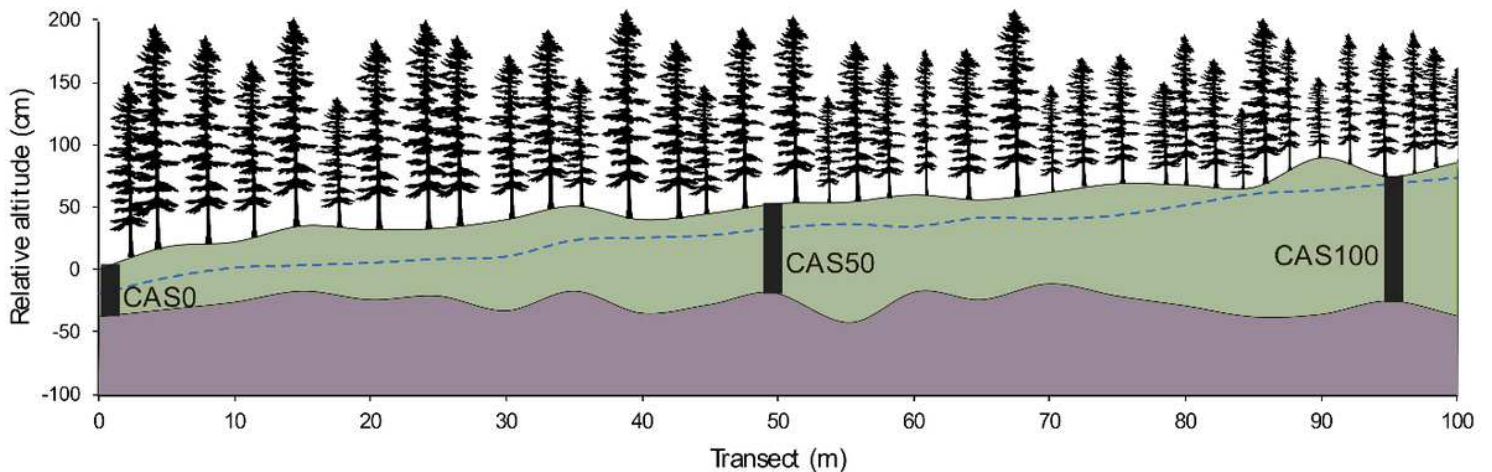
Figure 2

Schematic of the three sites along the study transect. Relative altitude of the organic layer (green) and the mineral surface (grey) are shown. Black rectangles represent the location of the sampled peat cores. The dotted blue line indicates the depth of the water table measured in the field. Trees are not to scale but are representative of variations in canopy openness along the transect.
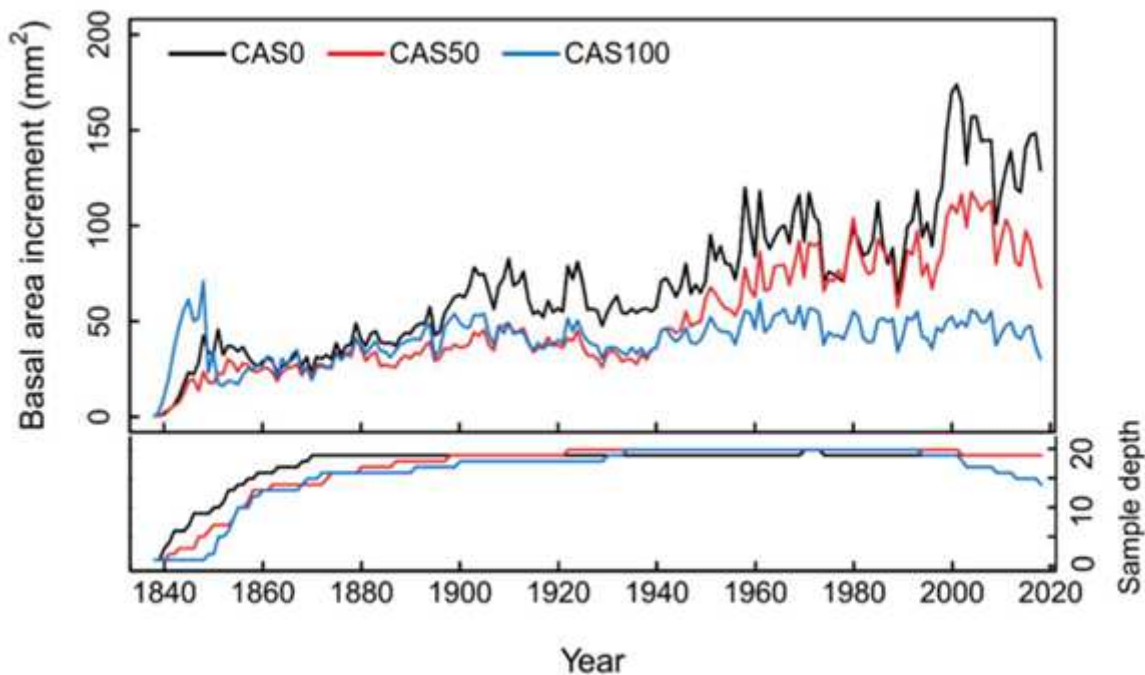
Figure 3

Mean annual basal area increment of black spruce trees since their establishment after the last fire event. The decrease in sample depth (n trees) at CAS100 since 2000 is explained by some trees for which the latest rings were partly absent. See Fig. S2.3 for BAI distribution.
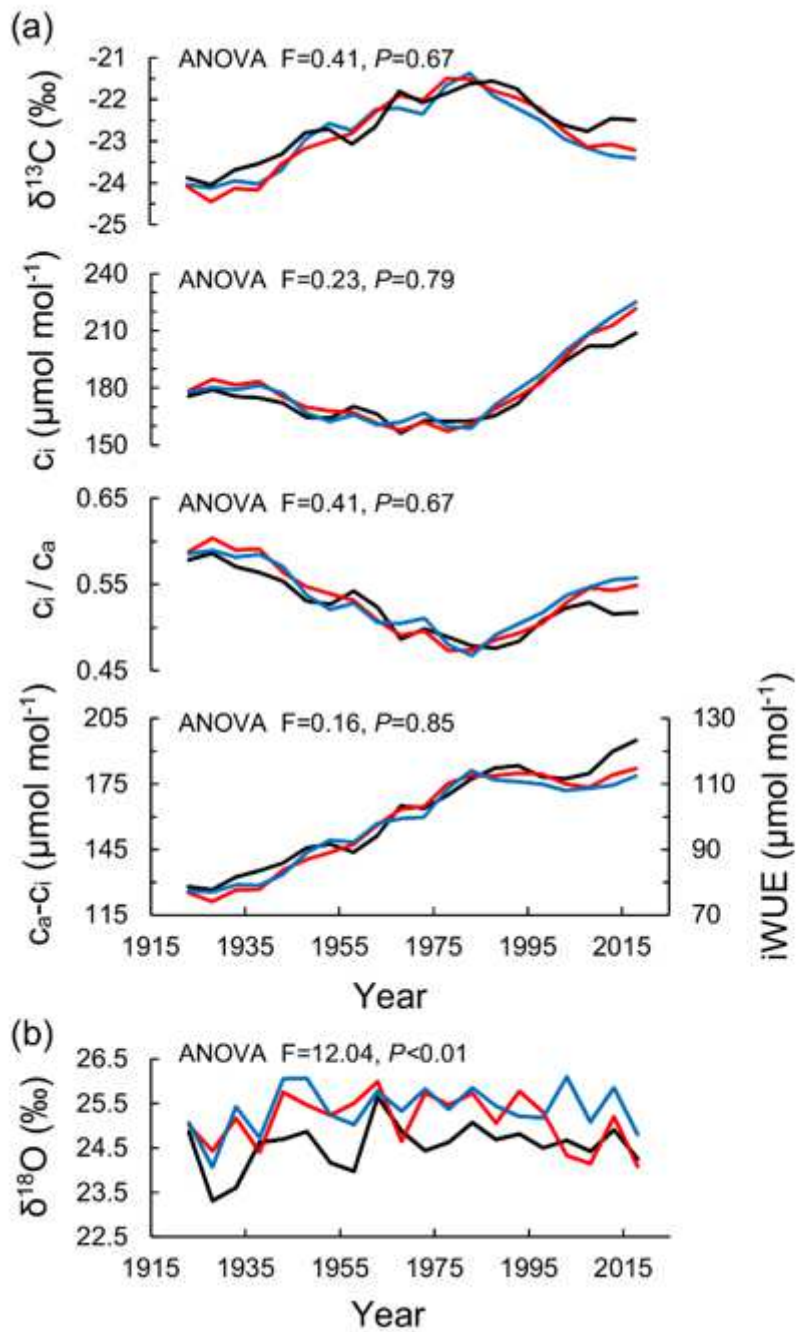
Figure 4

Black spruce ecophysiological response to rising c☐ based on five-year resolution δ13C and δ18O analyses for the period 1919-2018. (a) Tree-ring δ13C and δ13C-derived ecophysiological parameter values (ci, ci/ ca, ca- ci, iWUE); (b) tree-ring δ18O values. Results from CAS0, CAS50, and CAS100 are shown in black, red, and blue, respectively.

Figure 5

(a) WTD reconstructions for the post-fire period based on testate amoeba records and (b) growing degree days (>0°C) from May to September in the study area for the period 1950-2013. Error bars of both WTD reconstructions and age-depth modelling are shown by pale thin lines. Climate data were extracted from McKenney et al. (2011). A 10-year loess smoothing is shown by the pink dashed line.